# Spatial expression of an mRNA encoding Tie2-agonist in the capillary endothelium of the lung prevents pulmonary vascular leakage

Katrin Radloff[1,*], Birgitt Gutbier[2,*], Charlotte Maeve Dunne[3,4], Hanieh Moradian[3,4], Manfred Gossen[3,4], Katharina Ahrens[2], Laura Keller[2], Yadon Wang[2], Akanksha Moga[1], Leonidas Gkionis[1], Oliver Keil[1], Volker Fehring[1], Daniel Tondera[1], Klaus Giese[1], Ansgar Santel[1], Jörg Kaufmann[1,#], and Martin Witzenrath[2,#]

[1] Pantherna Therapeutics GmbH, 16761 Hennigsdorf, Germany

[2] Department of Infectious Diseases and Respiratory Medicine, Charité-Universitätsmedizin Berlin, corporate member of Freie Universität Berlin and Humboldt-Universität zu Berlin, 10117, Berlin, Germany

[3] Institute of Active Polymers, Helmholtz-Zentrum Hereon, 14513 Teltow, Germany

[4] Berlin-Brandenburg Center for Regenerative Therapies (BCRT) Charité Campus Virchow Klinikum, 13353 Berlin, Germany

[*] Authors contributed equally to this work

[#] Corresponding authors

## Abstract

Angiopoietin ligands Ang1 and Ang2 and the Tie2 receptor tyrosine kinases form an endothelial signaling pathway regulating vascular homeostasis and controlling vessel permeability, inflammation and angiogenic responses. Whereas Ang1-mediated Tie2 activation reduces inflammation and endothelial permeability, its antagonist, Ang2 increases it. Increased plasma Ang2 levels are associated with poor outcomes in patients with acute lung injury (ALI), as well as in acute respiratory distress syndrome (ARDS).

In the study presented here we tested the effect of a novel synthetic, nucleoside-modified mRNA-76 encoding for a hyperactive Ang1 derived fusion protein (COMP-Ang1) on attenuating post-inflammation vascular leakage. COMP-Ang1 mRNA was formulated into a cationic lipid nanoparticle (cLNP) using an optimized mixture of three different lipids and a microfluidic mixing technology. After intravenous injection, the respective mRNA-loaded LNPs were found to be delivered predominantly to the endothelial cells of the lung, while sparing other vascular beds. Also, the specific multimeric folding of the COMP-Ang1 protein complex appeared to be pivotal for its activity in preventing vascular leakage and in restoring the alveolar-endothelial barrier function in the inflamed and injured pulmonary vasculature. The mode of action of mRNA-76, such as its activation of the Tie2 signal transduction pathway, was tested by pharmacological studies *in vitro* and *in vivo* by systemic administration in respective mouse models. mRNA-76 was found to prevent lung vascular leakage/lung edema as well as neutrophil infiltration in an LPS-challenging model.

## Introduction

Acute respiratory distress syndrome (ARDS) is a life-threatening medical condition of respiratory failure characterized by rapid onset of widespread inflammation in the lungs. ARDS affects approximately 200 000 patients each year in the United States, and mortality and morbidity continues to be significant, remaining between 34.9 % and 40 %, depending on severity (Meyer et al. 2021; Matthay et al. 2019), resulting in nearly 75 000 deaths annually. Despite great improvements in management and heightened research efforts, ARDS still accounts for 10 % of intensive care unit (ICU) admissions globally, corresponding to more than 3 million patients with ARDS annually. ARDS can be caused by a variety of pulmonary (e.g., pneumonia, aspiration) or non-pulmonary (e.g., sepsis, pancreatitis, trauma) insults, leading to the development of nonhydrostatic pulmonary edema (Fan et al. 2018). Clinically, the syndrome is characterized by an acute developing, diffuse inflammatory lung injury initiated by increased alveolar capillary permeability, eventually resulting in increased lung weight, hypoxia (Fan et al. 2018) and fluid and neutrophil accumulation in the alveoli, which cannot be explained by hydrostatic edema. Primary treatment involves mechanical ventilation with low tidal volume together with treatments directed at the underlying cause, such as administering of antibiotics and fluid conservative strategies (Keddissi et al. 2019). However, to date there is no medication available for treatment and to further reduce ARDS mortality in patients. Hence there is a substantial medical need for novel and effective treatment approaches for ARDS, particularly in view of the significantly increased patient numbers affected by this life-threatening medical condition since onset of the worldwide “Covid-19” pandemic.

In ARDS, an initial vascular endothelial and alveolar epithelial cell activation or insult triggers massive liberation of inflammatory mediators, including complement activation products, cytokines, chemokines, proteases, and oxidants (Dolinay et al. 2012; Aranda-Valderrama and Kaynar 2018) which subsequently cause lung edema, a flooding of the lungs, thus impairing oxygen and carbon dioxide gas exchange of the lung capillaries. Albeit the inflammatory mediators recruiting immune cells, it is exactly their overabundance which eventually leads to a disruption of the endothelial barrier (vascular leakage) and to damage within the epithelial barriers in the alveolus. The endothelial angiopoietin (Ang)-Tie2 growth factor receptor pathway regulates vascular permeability and pathological vascular remodeling (Saharinen et

al. 2017b). Ang1 and Ang2 are both multimeric ligands for the receptor tyrosine kinase Tie2. In particular, the inactivation of Tie2 signaling due to an inflammatory increase in Ang2 secretion is regarded to be one of the major molecular mechanisms for the impairment of barrier function in the lung vasculature. Conversely, activation by Ang1 of Tie2 signaling restores endothelial barrier function and prevents further vascular leakage. This unique function of the Ang-Tie2 pathway in vascular stabilization renders this pathway an attractive and validated target in conditions such as ARDS, sepsis, macular edema, and cancer (Saharinen et al. 2017a).

Antibodies specific for Ang2 have been employed to prevent microvascular endothelial barrier dysfunction and to attenuate vascular remodeling and inflammation in a chronic lung infection model (Tabruyn et al. 2010). However, an Ang2 neutralization dependent restoration of basal Tie2 phosphorylation has not been shown so far. The second promising therapeutic approach to overcome Ang2 repression of the normal Tie2 signaling pathway has been to drive Tie2 activation to supra-physiological levels using recombinant Ang1 protein itself as well as derivatives thereof, such as COMP-Ang1 (Cho et al. 2004a) or CMP-Ang1 (Khan et al. 2021; Cho et al. 2004b). Additionally, either an unrelated agonist such as *Vasculotide* (Wu et al. 2015; Gutbier et al. 2017) or administration of cells expressing Ang1 (McCarter et al. 2007) were shown to be applicable and effective to that purpose. The approach to prevent and restore vascular barrier function by directly utilizing Ang1 proteins or derivatives has been hindered so far by the inherent predisposition of Ang1 to form higher order complexes for it to be catalytically active. Also, multimerization of Ang1 displays unfavorable pharmacokinetics. Highly oligomeric native Ang1 variants are, however, difficult to produce, purify and store in a stable and active form, and hence production in their multimeric form under GMP conditions has not been possible for clinical use so far.

Recombinant COMP-Ang1 is a fusion protein comprised of the multimerization domain of the rat cartilage oligomeric matrix protein (COMP) combined with the fibrinogen-related domain of human Ang1, and has been described previously as a hyperactive Tie2 agonist (Cho et al., 2004).

Here, we describe the mRNA-based approach of directed expression and secretion of a hyperactive Ang1 derivative, hCOMP-hAng1 fusion protein, to transiently activate the Tie2 pathway *in vitro* and *in vivo*.

## Materials & Methods

### mRNA synthesis

Codon-optimized mRNAs encoding human Ang1, COMP-Ang1, CMP-Ang1, Tie2 and NanoLuc proteins were synthesized and purified by BioSpring (Germany). Each mRNA was initiated with a cap, followed by a 5' untranslated region (UTR), a signal peptide sequence, an open-reading frame (ORF) encoding Ang1, COMP-Ang1, CMP-Ang1 and Tie2, a 3' UTR and a polyadenylated tail. Uridine was globally replaced with 1-methylpseudouridine.

### Cell transfection *in vitro*

Hela cells were transfected with mRNAs using Lipofectamine MessengerMax (Invitrogen, cat. #LMRNA001) according to manufacturer's protocol. Briefly, cells were seeded in 150 $cm^2$ culture flasks (TPP, cat. #90151) at 50 % confluency in serum-free DMEM (Gibco, cat. #61965-026). 15 h later, cells were transfected for 2 h with indicated amounts of MessengerMax-formulated mRNAs according to manufacturer's protocol. Transfection media was removed and replaced with fresh serum-free DMEM for indicated time points. After 24 h, the supernatant was removed (around 25 ml) and either concentrated 10-fold with Amicon 3 kDa spin columns (Merck, cat. #UFC900308) and brought to a final volume of 2 ml for subsequent Western blot analysis (Fig.1B, C) or directly used for Tie2 activation studies (Fig. 2A, B, Fig. 3B). Human pulmonary microvascular endothelial cells (HPMEC) (Promocell, cat. #C-12281) were seeded onto 6-well plates (Thermo Scientific, cat. #140675) and left for 3 days until 100 % confluency in full supplemented ECM MV2 cell media (Promocell, cat. #C-22022). 15 h before transfection was placed in serum-reduced ECM MV2 media (containing 10 % of originally cell growth supplement MV2). Cells were transfected with preformulated mRNA-LNP at indicated concentrations in serum-free ECM media for 2 h. After transfection, media was replaced with serum-reduced ECM MV2 and left for indicated time points.

### Western Blot analysis

Cells were washed with ice-cold phosphate buffered saline (PBS) twice and lysed with ice-cold RIPA buffer (Thermo Scientific, cat. #89901) supplemented with Halt™ Protease and Phosphatase Inhibitor Cocktail (Thermo Scientific, cat. #78441). Tissue samples were solubilized in T-PER™ Tissue Protein Extraction Reagent (Thermo Scientific, cat. #78510)

134 supplemented with Pierce Protease and Phosphatase Inhibitor tablets (Thermo Scientific, cat.
135 #A32958) using Qiagen TissueLyser LT (Qiagen, cat. #69980). A mixture of cell or tissue lysate,
136 50 mM dithiothreitol NuPAGE reducing agent (Invitrogen, cat. #NP0009) and NuPAGE sample
137 buffer (Invitrogen, cat. #NP0007) were heated at 70 °C for 10 min, electrophoresed in NuPAGE
138 4–12 % Novex Bis-Tris Gels and MOPS buffer (all from Invitrogen, cat. #NP0335BOX, NP0001)
139 and transferred to nitrocellulose membrane (Cytiva, cat. #10600003; NuPAGE™ Transfer
140 Buffer (Invitrogen, cat. #NP00061). After a 60 min blocking step (Intercept® Blocking Buffer;
141 LiCor, cat. #927-60001) membranes were washed with Tris Buffered Saline with Tween® 20
142 (CST, cat. #9997S) probed at 4 °C overnight with specific primary antibodies diluted in
143 Intercept Antibody Diluent (LiCor, cat. #927-65001). Binding of primary antibodies was
144 detected by near infrared IRDye secondary antibodies (LiCor, cat. #926-32213, 926-32214,
145 926-68072) and near infrared signals were analyzed using LiCor Odysee CLx. Band intensities
146 were analyzed using Empiria Studio Software 2.1.0134 (LiCor). Primary antibodies used:
147 Angiopoeitin 1 (abcam, cat. #ab183701), human Tie2 (CST, cat. #7403), mouse Tie2 (Merck,
148 cat. #05-584), pY992 Tie2 (R&D Systems, cat. #AF2720), Akt (CST, cat. #9272 and #2920S),
149 pS473 Akt (CST, cat. #4060), S6K (CST, cat. #9202), pT389 S6K (CST, cat. #9234), FoxO1 (CST,
150 cat. #2880), pT389 FoxO1 (CST, cat. #9461).
151
152 **Immunoprecipitation**
153 Anti-Tie2 antibody ab33 (R&D Systems, Merck, cat. #05-584) for Tie2 IP or Tie2-Fc fusion
154 protein (R&D Systems, cat. #313-TI) for COMP-Ang1 IP were covalently coupled to M-270
155 Epoxy Dynabeads™ (Thermo Scientific), cat. #14311D) at a ratio of 15 µg protein per mg
156 Dynabeads according to manufacturer's protocol. Briefly, 1.5 mg of antibody-coupled beads
157 were incubated with tissue lysates overnight at 4 °C. Beads were washed 5 times with 1 ml
158 with ice-cold RIPA buffer and finally denaturated using 1x NUPAGE loading dye containing 1x
159 NUPAGE reducing agent (all Thermo Scientific). Beads were removed and lysates were
160 analyzed by Western blotting analysis.
161
162 **Fluorescent microscopy**
163 HPMEC were seeded in Chamber Slides (NUNCTM Lab-TekTM, cat. #154534PK) at
164 $1x10^5$ cells/ml in endothelial MV2 growth medium. Cells were incubated for 3-5 days at 37°C
165 in 5 % $CO_2$. Cells were washed 2 times with pre-warmed PBS (Thermo Scientific, cat. #14190),

166 final PBS wash was replaced with endothelial MV2 basal medium devoid of serum and
167 supplements. Formulations containing mRNA were diluted in basal medium and added to each
168 well for a final concentration of 0,38 ng/well. Cells were returned to the incubator for a further
169 2 hours. Media containing formulations was removed and replaced with 10 % MV2 growth
170 medium for 16 h. For TNFα treatment, 10 % MV2 growth medium with TNFα (R&D Systems,
171 cat. #210-TA) or vehicle was spiked into each well for a final concentration of 10 ng/ml for a
172 further 6 h. Cells were fixed in 4 % PFA (Thermo Scientific, cat. #15670799) for 10 min at room
173 temperature (RT). Cells were permeabilized in PBS containing 0.02 % Triton-X (PBS-T) for 2x
174 10 min washes on a rocker at RT. Primary antibody mix was made up with rabbit anti-VE-
175 Cadherin (CST, cat. #2500) diluted at 1:400 in 2 % donkey immunobuffer containing 0.02 %
176 Triton-X, rocking at 4 °C overnight. Primary antibodies were removed and washed in PBS-T 2x
177 10 min on a rocker at RT. Secondary antibody mix was made up with donkey anti-rabbit (H+L)
178 highly cross-adsorbed Alexa FluorTM 647 (Thermo Scientific, cat. #A-31573) diluted at 1:400
179 and Alexa FluorTM 594 Phalloidin (Thermo Scientific, cat. #A12381) at 1:2000 in 2 % donkey
180 immunobuffer containing 0.02 % Triton-X rocking at RT for 5 h. Cells were washed in PBS-T for
181 a further 2x 10 min at RT. Nuclear staining was carried out with Hoechst (Tocris, cat. #5117)
182 diluted at 1:500 in PBS for 15 min, followed by a final PBS-T wash. Fluorescent images were
183 acquired with a Nikon Eclipse Ti-U with an ELWD S Pan Fluor 40X/0.6 objective lens. Images
184 were processed using ImageJ (Schneider et al., 2012).
185
186 **Transcellular electrical resistance of human pulmonary microvascular endothelial cells**
187 HeLa cells were first treated for 24 h with LNP-formulated mRNA-76 or with a Luciferase mRNA
188 (see above) in order to generate conditional serum-free DMEM medium containing secreted
189 COMP-Ang1 or secreted luciferase. Moreover, HPMEC were grown to confluency on
190 evaporated gold microelectrodes (8-well array with ten electrodes per well, (ibidi GmbH, cat.
191 #72010) and connected to an Electrical cell-substrate impedance sensing system (ECIS;
192 Applied Biophysics, Troy, NY) (Tiruppathi et al. 1992; Giaever and Keese 1993) to enable
193 continuous monitoring of transcellular electrical resistance (TER) (Mitchell et al. 1989). After
194 monitoring baseline readings for 60-90 min, HPMEC medium was mixed 1:10 with the
195 conditional HeLa media (COMP-Ang1 supernatant or Luc supernatant) for 30 min or for 60 min
196 before treatment with three different concentrations of pneumolysin (PLY; 0.25, 0.5 and
197 1.0 µg/ml) (Mitchell et al. 1989) to evoke a barrier failure in HPMEC. TER values from each

198 microelectrode were continuously monitored for 5 hours after PLY stimulation and normalized
199 as the ratio of measured resistance to baseline resistance. The area under the curve (AUC)
200 was calculated from start of PLY stimulation on.
201
202 **Animals**
203 Female C57BL/6N mice (8 to 10 weeks, 18 to 20 g; Charles River, Sulzfeld, Germany) were used
204 for all experiments. All animal experiments were approved by institutional and governmental
205 German authorities ("Tierschutzbeauftragte" (animal welfare officer) and
206 "Tierschutzausschuss" of Charité–Universitätsmedizin Berlin; and by the Landesamt für
207 Gesundheit und Soziales Berlin; approval ID A0179/20), and were in accordance with the
208 Federation of European Laboratory Animal Science Associations (FELASA) guidelines and
209 recommendations for the care and use of laboratory animals (equivalent to American ARRIVE).
210 Mice were randomly assigned to the appropriate experimental groups and were kept in
211 closed, individually ventilated cages with filter hoods (type II-L, ZOONLAB), under specific
212 pathogen-free conditions, with free access to food and water, room temperature between 20
213 and 22 °C, air humidity between 50 and 65 % and 12 h light/dark cycle.
214
215 **Transfection in vivo and isolated perfused and ventilated mouse lung (IPML) experiments**
216 Intravenous tail vein administration (slow 100 µl bolus tail vein injection) with either
217 Luciferase-mRNA (2 mg/kg) or mRNA-76 (2 mg/kg, 1.5 mg/kg or 1 mg/kg) was performed 6 h
218 or 15 h before the experiment in the isolated mouse lung model was started. Subsequently,
219 mice were anesthetized, placed in a 37 °C heated chamber ("artificial thorax"),
220 tracheotomized and ventilated as described (Von Bethmann et al. 1998). After laparotomy,
221 final blood collection via the vena cava, sternotomy, and cannulation (pulmonary artery, left
222 atrium), lungs were perfused with Krebs-Henseleit-hydroxyethylamylopectine buffer (Serag-
223 Wiessner) supplemented with sodium bicarbonate (1:50). The chamber was closed, and lungs
224 were ventilated by negative pressure (Pexp -4.5, Pins -9.0 cm $H_2O$) and perfused (1 ml/min)
225 for 20 min to establish baseline conditions. Then 0.04 % human serum albumin (HSA; 20 %
226 solution; CSL Behring, cat. #Human-Albumin 20 % Behring) was admixed continuously to the
227 perfusate 10 min prior to intravenous bolus application of recombinant pneumolysin (PLY;
228 1.4 µg/ml) (Mitchell et al. 1989). Thirty minutes after PLY challenge, bronchoalveolar lavage
229 (BAL) was performed (2 x 650 µl, 0.9 % saline buffer), and HSA concentration was measured

230 in BAL fluid (BALF) via ELISA (Bethyl Laboratories, cat. #E88-129) in order to quantify the lung
231 barrier failure (Seybold et al. 2005; Witzenrath et al. 2006).
232
233 **Neutrophilia transmigration experiment**
234 Animals (n=10) were challenged intratracheally with 0.9 % w/v saline or with LPS (3 mg/kg).
235 Two hours later animals were treated with mRNA-76-cLNP or with control $mRNA^{LUC}$-cLNP
236 employing a dosage of 1.5 mg/kg via intravenous tail vein injection. Control group animals
237 received intraperitoneal injections of Dexamethasone (3 mg/kg) one hour prior to, and 8
238 hours after LPS administration. Animals were sacrified after 24 hours and the airway lavaged
239 with 0.3 ml of PBS using an inserted cannula. The bronchoalveolar lavage from each mouse
240 was centrifuged at 1000 g for 10 min at ca 4 °C. The cell pellet was re-suspended in 0.5 ml PBS
241 and retained on wet ice until analysis. A total and differential cell count of the BALF
242 supernatant was performed using the XT-2000iV (Sysmex UK Ltd). The samples were vortexed
243 for approximately 5 seconds and analyzed. Total and differential cell counts (including
244 neutrophils, lymphocytes and mononuclear cells (includes monocytes and macrophages))
245 were measured as number of cells per animal.
246

247 ## Results

248 Expression of coding sequences of the wild-type human Ang1 and of engineered fusion
249 proteins COMP-Ang1 and CMP-Ang1 flanked by heterologous untranslated regulatory
250 sequences was tested in cell culture systems in order to identify a potent mRNA construct for
251 Tie2 activation. Wildtype human Ang1 mRNA with heterologous UTRs served as a control next
252 to either a construct with an ORF for a COMP-Ang1 fusion protein or a construct containing
253 an ORF with a CMP-Ang1 fusion protein (**Fig. 1A**). Similar COMP-Ang1 and CMP-Ang1
254 recombinant fusion proteins have been previously described which contain the rat homologue
255 of COMP or human CMP as potent Tie2 agonist in *in vitro* assays and in mouse models (Cho et
256 al. 2004b; Oh et al. 2015; Wallace et al. 2021).
257

258 **mRNA directs transient expression of human Ang-1 and COMP-Ang1 and CMP- fusion**
259 **proteins *in vitro***

260 *mRNAs* encoding wildtype human Ang1, fusion proteins COMP-Ang1 and CMP-Ang1 were
261 transfected into HeLa cells using Lipofectamine MessengerMax. Cell culture supernatants
262 were collected 3 h, 6 h and 24 h after the transfection, and corresponding whole cell lysates
263 were prepared. The supernatants and cell lysates were subsequently analyzed by
264 immunoblotting employing an Ang-1 specific antibody. A strong protein expression signal was
265 detected for all three constructs, and protein levels post-transfection of the mRNA construct
266 were found to be higher than those of endogenous Ang-1 protein (**Fig. 1B**). Equivalent protein
267 levels were detected in the supernatant of the cell culture, indicating secretion of the
268 expressed proteins (**Fig. 1C**). Multimerization potential of the expressed Ang1 derivates was
269 analyzed by employing non-reducing PAGE on the supernatant. Contrary to CMP-Ang1, the
270 COMP-Ang1 fusion protein was found to be capable of forming higher-order (pentameric)
271 homopolymers (**Fig. 1D**).
272

273 **Activation of Tie2 by COMP-Ang1 and CMP-Ang1**

274 The chimeric COMP-Ang1 derivative encoded by mRNA-76 was found to *in vitro* activate Tie2
275 in a paracrine manner. Tie2-negative HeLa cells were first transfected for 24 h with *mRNA*
276 encoding for Tie2 receptor using Lipofectamine MessengerMax. Subsequently, cells were
277 incubated for 15 min or 30 min with supernatants from HeLa cells previously transfected for
278 24 h with mRNA encoding the different Ang1 derivatives, or with NanoLuc-encoding control
279 mRNA using Lipofectamine MessengerMax. Ensuing, Tie2-transfected HeLa cells were lysed
280 and protein levels analyzed by Western blotting. Both supernatants with Ang1 derivatives
281 displayed a significantly stronger activation of the Tie2 receptor as assessed by phospho-Y992
282 Tie2 antibody (**Fig. 2A**) than when activated by the Luc-control and wildtype Ang1 proteins.
283 Ability of different Ang1-derivatives to induce paracrine activation of the Tie2 pathway in
284 human primary endothelial cells was then investigated in a second set of experiments. For
285 this, starved primary HPMECs (human primary microvascular endothelial cells) were
286 incubated for 10 and for 30 min with supernatants from HeLa cells previously transfected in
287 serum-free medium for 24 h with mRNAs encoding the different Ang1 derivatives using
288 Lipofectamine MessengerMax, or with NanoLuc as a control. HPMEC cells were lysed after 10
289 and 30 min, and phosphorylation status of Tie2, Akt and S6K analyzed by Western blotting and

290 compared to lysates from starved cells or from cells stimulated for 10 and 30 min with FCS
291 (**Fig. 2B**). Strongest downstream activation of Akt and S6K was seen with FCS treatment on
292 starved cells, thus corroborating the expected broad growth factor response. Cells treated
293 with supernatant from HeLa cells transfected with mRNA-76 encoding COMP-Ang1 also
294 showed robust phosphorylation of Akt and of S6K, but additionally exhibited
295 autophosphorylation of Tie2, indicative for a more specific pathway activation. The paracrine
296 effect of HeLa conditional medium-derived COMP-Ang1 resulted in a better Tie2 pathway
297 activation as compared to CMP-Ang1, leading to selection of mRNA-76 /COMP-Ang1 for the
298 following experiments. mRNA-76 encoding COMP-Ang1 was directly transfected into HPMEC
299 and secretion and Tie2 signaling was analyzed in order to demonstrate increased autocrine
300 Tie2 activation. Strong COMP-Ang1 expression was observed in cell lysates and in the
301 supernatant of the respective culture, indicating efficient secretion (**Fig. 2C**). Lysate analysis
302 of serum-starved HPMEC transfected with mRNA-76 revealed phosphorylation of Tie2, Akt
303 and FOXO1, thereby indicating functional Tie2 pathway activation at 4 h and 8 h post-
304 transfection, as well as fast onset of activation. Waning of Tie2 receptor activation and a
305 reduction of Tie2 receptor protein was observed at 24 h and 48 h post transfection, consistent
306 with previous reports describing a ligand dependent Tie2 internalization and degradation
307 (Bogdanovic et al. 2006; Ghosh et al. 2016; Wehrle et al. 2009) as well as reduced expression
308 of Tie2 mRNA upon Ang1 treatment (Hashimoto et al. 2004).
309
310 **COMP-Ang1 expression stabilizes endothelial barrier function *in vitro***
311 Regulation of endothelial barrier stabilization by Ang1/Tie2 signaling has been shown to be
312 mediated by VE-Cadherin-dependent cell-cell adhesion and cortical actin formation, since the
313 cytoplasmatic tail of VE-cadherin is known to contain several phosphorylation sites with
314 different distinctive and selective effects on endothelial cell function (Hellenthal et al. 2022).
315 However, inflammatory conditions lead to disruption of VE-Cadherin complexes by
316 phosphorylation-dependent internalization and by degradation, as well as to formation of
317 actin stress fibers. We analyzed VE-Cadherin distribution in HPMEC cells upon TNF$\alpha$ challenge
318 by immunofluorescence staining and by microscopy analysis.
319 As reported previously (Xia et al. 1998), TNF$\alpha$ was shown to induce disruption of cell-cell
320 adhesion as verified by disruption intercellular VE-Cadherin staining (**Fig. 3A**, arrows) and by
321 formation of actin stress fibers in non-transfected cells (UT) as well as in cells transfected with

322 control mRNA$^{LUC}$-cLNP. However, cells transfected with mRNA-76-cLNP displayed more VE-
323 Cadherin staining even if unstimulated but in the presence of TNF$\alpha$. This observation argues
324 for the existence of increased VE-Cadherin trans-interaction area at overlapping cell edges, as
325 previously also described by Birkuva *et al*. (Birukova et al. 2012).
326 Following demonstration of functional Tie2 activation on VE-Cadherin complex stabilization,
327 we investigated the potential effect of mRNA-76 directed expression of COMP-Ang1 on
328 pneumolysin-evoked barrier failure in cell culture. Recovery of the pneumolysin-evoked
329 barrier failure was measured by monitoring transcellular electrical resistance (TER) (Srinivasan
330 et al. 2015). TER measurements are performed by applying an AC electrical signal across
331 electrodes placed on both sides of a cellular monolayer and subsequently measuring voltage
332 and current to calculate the electrical resistance of the barrier (Elbrecht et al. 2016). A
333 significantly improved transcellular electrical resistance was observed with the mRNA-76
334 conditional medium at lowest pneumolysin concentration of 0.25 µg/ml, but not with the
335 supernatant form HeLa cells transfected with Luciferase mRNA (**Fig. 3B,** purple lines: COMP-
336 Ang1 dotted line, Luciferase supernatant solid line). This effect was observed in pneumolysin-
337 induced barrier failure experiments after pretreatment with conditional supernatant for
338 30 min or 60 min. These data indicate that mRNA-76 treatment leads to expression and
339 secretion of COMP-Ang1 and the so expressed COMP-Ang1 is functional in a paracrine manner
340 on microvascular endothelial cell (HPMEC) monolayers as demonstrated by its ability to
341 attenuate the PLY-induced TER decrease. These findings confirm the proposed mode of action
342 of our COMP-Ang1 molecule in diminishing inflammation induced hyperpermeability via its
343 respective activation of the Tie2 signaling pathway.
344
345 **mRNA-76 enables COMP-Ang1 expression and Tie2 pathway activation in mice**
346 Various physical characteristics of LNPs affect organ biodistribution and cell specificity of the
347 mRNA delivery, namely size, surface charge, pKa of the lipids, lipid composition and
348 mRNA/lipid ratio, PEGylation (Eygeris et al. 2022; Hou et al. 2021; Kauffman et al. 2016;
349 Kowalski et al. 2019). We show that our mRNA-76 formulated in cationic lipid-nanoparticles
350 (cLNPs) enable Tie2 activation by paracrine and autocrine COMP-Ang1 expression *in vivo.* Our
351 cationic LNP formulations are based on lipoplex formulations previously described, for siRNA
352 *in vivo* delivery to the pulmonary endothelium (Fehring et al. 2014; Gutbier et al. 2018; Santel
353 et al. 2006b, 2006a). Expression of mRNA-76 directed COMP-Ang1 was analyzed by Western

354 Blot of protein from lung tissue from mice (n=4) treated by intravenous tail vein administration
355 with 2 mg/kg mRNA-76-cLNP. Robust COMP-Ang1 expression was detected in lung lysates
356 from mice 6 h after treatment, and declining expression levels were observed in mice 24 h
357 post treatment due to the transient nature of mRNA (**Fig. 4A**). As expected from previous
358 studies with cationic LNPs, mRNA-76-cLNP mediated robust lung tissue-selective COMP-Ang1
359 expression, while inducing no significant COMP-Ang1 expression in tissue lysates from heart,
360 liver, spleen, and kidney (**Fig. 4B**). Immune-precipitation was performed on different organ
361 lysates using Tie2-Fc fusion protein for capturing of COMP-Ang1 to confirm lung selective
362 COMP-Ang1 expression. Even with this more sensitive detection method the predominant
363 COMP-Ang1 expression was observed in lung lysates, with some minor expression also seen
364 in the spleen (**Fig. 4C**). No significant expression of COMP-Ang1 was detected in liver, heart
365 and kidney thus confirming the selective pulmonary delivery of mRNA-76-cLNP.
366
367 **Single-cell transcriptomics of murine lungs after mRNA-76-cLNP treatment**
368 We performed single-cell RNA-sequencing on cells derived from murine lungs in order to
369 characterize the specific cell types with mRNA-76 uptake. Lungs from two mice treated with
370 1.5 mg/kg mRNA-76-cLNP (2 h post administration) were obtained, and lung cell suspension
371 was subjected to droplet-based single-cell gene expression profiling (**Fig. 5A**). We obtained
372 5,100 high-quality transcriptome readings and were able to identify 13 cell clusters with main
373 cell types of the respective lung samples by employing dimensionality reduction via t-
374 distributed stochastic neighbor embedding (t-SNE) and graph-based clustering (**Fig. 5B**).
375 We observed mRNA-76 reads to be largely restricted to cluster 8 and cluster 10, representing
376 cells of the alveolar capillary endothelium (gCap, general capillary cells) and aCap (alveolar
377 capillary cells) recently termed aerocytes (Gillich et al. 2020), as well as monocytes,
378 respectively. Minor amounts of mRNA-76 appeared to also be present in a sub-cluster of the
379 pulmonary neutrophils (cluster 11). We analyzed the mRNA reads of Tie2 and VE-cadherin,
380 both being endothelial cell specific expressed genes, in order to confirm the endothelial
381 specific clustering for mRNA-76 into cluster 8. The overlap with the reads for both markers
382 confirmed cell type specificity of mRNA-76 delivery (**Fig. 5D**). In contrast to mRNA-76,
383 endogenous Ang1 mRNA is mainly detected in cluster 6, which does not overlap with reads
384 for the Tie2 receptor mRNA (**Fig. 5E**). The observed cell type-specific expression profiles

385 suggest a paracrine Tie2 activation for the endogenous Ang1, as well as a potential autocrine
386 Tie2 activation by ectopically expressed, mRNA-76-encoded COMP-Ang1.
387
388 **mRNA-76 mediated Tie2 pathway activation in murine lungs**
389 We then demonstrated Tie2 pathway activation in lung tissue to be induced by mRNA-76
390 COMP-Ang1 expression in murine lung tissue. Activation of PI3 kinase signaling including Akt
391 phosphorylation is known to be a downstream effect of Tie2 receptor activation. Of note,
392 demonstrating COMP-Ang1 mediated activation of Tie2 signaling is difficult due to the low
393 proportion of Tie2-expressing endothelial cells within total lung lysates in healthy, non-
394 inflamed lungs. Therefore, Tie2 was immuno-precipitated from lung tissue lysates of mice
395 previously treated with mRNA-76 using Tie2-specific antibodies. Tie2 phosphorylation of the
396 lung was subsequently shown by Western blot analysis of immuno-precipitated samples using
397 anti-phospho-Tie2 antibody (p*Y992) (**Fig. 6A**). Signal quantification of phosphorylated Tie2
398 was performed using LiCor Odyssee CLx and measured relative to corresponding total Tie2
399 levels. In addition, immunoblot analysis using Ang1-specific antibodies showed co-
400 immunoprecipitation of COMP-Ang1 thus demonstrating efficient binding of human COMP-
401 Ang1 to murine Tie2. Since Akt phosphorylation upon COMP-Ang1 stimulation is mediated by
402 Tie2 activation, whole lung tissue lysates from mice treated with 1.5 mg/kg mRNA-76-cLNP
403 were analyzed for COMP-Ang-1 expression, Akt expression and Akt-phosphorylation by
404 immunoblot (**Fig. 6B**) in comparison to control lysates (Saline treated). Akt phosphorylation
405 levels were shown to be highest 6 h post mRNA-76-cLNP treatment.
406
407 **mRNA-76 treatment reduces pneumolysin-evoked vascular permeability in an isolated**
408 **perfused and ventilated mouse lung (IPML) model for vascular leakage**
409 A pneumolysin (PLY) stimulation experiment was performed on isolated and ventilated mouse
410 lungs (IPML model) to demonstrate mRNA-76 efficacy in preventing and/or decreasing lung
411 hyperpermeability by inflammation (**Fig. 7A**). In the employed IPML model, PLY stimulation
412 increases lung permeability 30 min after application, as described previously (Gutbier et al.
413 2017; Witzenrath et al. 2006). Here, treatment with mRNA-76 significantly decreased
414 pneumolysin-induced hyperpermeability of mouse lungs as compared to treatment with
415 Luciferase (**Fig. 7B**). Dose dependent reduction of HSA levels in the BALF was observed at 6 h
416 and 15 h post mRNA-76 treatment as compared to that derived from control mice, indicating

reduced vascular leakage. These results suggest that mRNA-76 pretreatment is effective in preventing pneumolysin-induced vascular leakage in the IPML model, and respective observations are consistent with the previously established mode of action of Tie2 activation by mRNA-76 directed expression of COMP-Ang1 in lung tissues. The effective dose in this mouse efficacy model is approx. 1 mg/kg for the 6 h time point and marginally higher at later time points (15 h). This decreasing effect on vascular leakage at later time points with lower doses suggests a more sustained expression with higher mRNA-76 dosing.

**mRNA-76 directed COMP-Ang1 expression reduces neutrophil influx after LPS challenge in murine lungs**

We observed a significant therapeutic effect on endotoxin/LPS induced neutrophilia after temporal and spatial expression of COMP-Ang1 in a murine model of endotoxin (*E. coli* lipopolysaccharide, LPS)-induced pulmonary inflammation (**Fig. 8A**). Hence, we detected a significant decrease in LPS induced neutrophil influx into the alveoli after single mRNA-76-cLNP treatment in our experimental model (**Fig. 8B**). The level of the decreased neutrophil influx effect is in the same range as that of prophylactic and therapeutic dexamethasone treatment used as positive control for this assay. No significant reduction regarding cell influx was observed with $mRNA^{Luc}$-cLNP as compared to vehicle control mice. Also, no changes in LPS induced vascular leakage (e.g., changes in wet lung weights) were observed with mRNA-76-cLNP treatment as compared to control mRNA formulation, indicating that vascular leakage and leucocyte emigration do not necessarily occur together in the blood vessels of the lung. The fact that elevated levels of circulating cytokines are not perturbed by enhancement of vascular integrity and hence the notion that leakage can be regulated distinctly from the inflammatory response has been discussed previously by others (Filewod and Lee 2019). Generally, the effect of mRNA-76-cLNP treatment in rodent models for LPS-induced lung injury could also be dependent on the time point at which samples are obtained, and at which respective physiological measurements are taken. The LPS model might therefore be not adequate to simultaneously address the question of both neutrophil efflux as well as lung edema at similar timepoints 24 h post endotoxin challenge, as opposed to the IPML model which was used primarily for experimentally reducing vascular leakage. In our in a murine model of LPS-induced pulmonary inflammation, intravenous mRNA-76-cLNP treatment showed a strong therapeutic effect in reducing leukocyte extravasation and/or transmigration

449 of neutrophils for the timepoint(s) analysed. Notably, leukocyte influx reduction and reduction
450 in edema formation might be clinically highly desirable to counteract delayed apoptosis of
451 parenchymal neutrophils, believed to contribute to tissue injury (Teder et al. 2002). Taken
452 together, our experiments in the IPML mouse model confirm a dose dependent therapeutic
453 effect of COMP-Ang1 on endothelial permeability, as well as a therapeutic efficacy on
454 dysregulated lung inflammation in the LPS-induced pulmonary neutrophilia mouse model.
455 Both underlying pathophysiological mechanism, loss of endothelial permeability and
456 dysregulated lung inflammation, are hallmark events of early ARDS syndrome.

457

458 **Discussion**

459 In our work presented here we introduce mRNA-76-LNP, a novel drug modality utilizing
460 mRNA-based expression technology, in combination with a lipid nanoparticle-based delivery
461 technology, to achieve transient and localized expression of functional Ang1 protein
462 derivatives in the lung vasculature. Our new approach and technology thus overcome the
463 limitations of efficaciously administering recombinant multimeric proteins for activating Tie2
464 signaling. In the past, a promising therapeutic approach to overcome Ang2 repression of the
465 normal Tie2 signaling pathway has been to drive Tie2 activation to supra-physiological levels
466 using recombinant Ang1 protein itself as well as derivatives thereof, such as COMP-Ang1 (Cho
467 et al. 2004a) or CMP-Ang1 (Khan et al. 2021; Cho et al. 2004b). Additionally, either an
468 unrelated Tie2 agonist such as *Vasculotide* (Wu et al. 2015; Gutbier et al. 2017) or applying
469 cell-based Ang1 gene therapy (McCarter et al. 2007) have been used to that purpose. The
470 approach to prevent and restore vascular barrier function by directly utilizing Ang1 proteins
471 or its derivatives has been hindered so far by the inherent predisposition of Ang1 to form
472 higher order complexes for it to be catalytically active, since Tie2 receptors only interact with
473 highly oligomeric Ang1. Also, multimerization of Ang1 displays unfavorable pharmacokinetics.
474 Highly oligomeric native Ang1 variants are, however, difficult to produce, purify and store in
475 a stable and active form, and hence production in their multimeric form under GMP conditions
476 has not been possible for clinical use so far. In addition Ang1, unlike Ang2, has been shown
477 previously by Xu *et al*. to be incorporated efficiently into the extracellular matrix (ECM) via its
478 linker peptide region explaining its rapid serum clearance (Xu and Yu 2001). Interestingly, only

479 COMP-Ang1 and CMP-Ang1 were detected in significant amounts in the cell supernatant (**Fig.**
480 **1**), despite similar expression levels in lysates of Hela cells transfected with the three Ang1
481 variants. One possible explanation for this observed difference might be that albeit the Ang1
482 linker domain being present in all three Ang1 variants, conceivably only wt-Ang1 interacts with
483 components of the ECM via its N-terminal multimerization domain. Moreover, COMP-Ang1
484 and CMP-Ang1 show a more robust Tie2 activation in Hela cells with high levels of ectopically
485 expressed Tie2, hence suggesting a superior paracrine activity of COMP-Ang1 and CMP-Ang1
486 as compared to wt-Ang1. In fact, paracrine Tie2 activation was demonstrated only with COMP-
487 Ang1 in HPMEC. COMP-Ang1 was shown to form solely pentamers, this being most likely due
488 to the presence of the COMP multimerization domain. In contrast, CMP-Ang1 was shown to
489 preferentially form dimers owing to the presence of its CMP dimerization domain (**Fig. 1D**).
490 Tie2 activation has been previously reported to require a specific distance of the Ang1 binding
491 domains in relation to the two Tie2 monomers (Leppänen et al. 2017). This very specific
492 steric/spatial interaction is potentially facilitated by the pentameric COMP-Ang1 as compared
493 to the dimeric CMP-Ang1 in low Tie2 expressing HPMEC cells. As a result ,the observed higher
494 and robust COMP-Ang1 mediated Tie2 activation in our system is most likely caused by its
495 higher solubility compared to wt-Ang1, as well as by its more efficient multimerization into
496 active pentamers as compared to that of CMP-Ang1. The difference in Tie2 activation (**Fig. 2**)
497 in our hands led us focus on mRNA-76 encoding COMP-Ang1 for our further experiments. We
498 subsequently demonstrated that mRNA-76 mediated COMP-Ang1 expression and Tie2
499 activation had phenotypic effects on cell adhesion by way of monitoring transcellular electrical
500 resistance in HPMEC monolayers (**Fig. 3**). This observed stabilization of endothelial barrier
501 function in *in vitro* cell culture is consistent with our *in vivo* results demonstrating a reduction
502 of pneumolysin-evoked permeability in isolated perfused and ventilated mouse lungs after
503 mRNA-76 treatment (**Fig. 6**). The underlying LNP formulation used in these experiments is
504 based on our previous experimental work with siRNA-lipoplex formulations (Fehring et al.
505 2014; Santel et al. 2006b, 2006a). Functional delivery of the mRNA-76 payload was shown to
506 occur in the lung vasculature, more specifically in pulmonary capillary endothelial cells (scRNA-
507 Seq **Fig. 5**). Hence, here the synthetic mRNA becomes translated and consequently respective
508 COMP-Ang1 is secreted as a multimer in order to bind and activate Tie2 receptors in a
509 presumably paracrine and autocrine rather than endocrine manner (**Fig. 4**). Our data
510 demonstrating COMP-Ang1 expression in mouse lung tissue together with *in vivo* mRNA-76

511 uptake by single cell transcriptional analysis and its subsequent Tie2 pathway activation in
512 moues lung tissue therefore demonstrate the projected mode of action of our novel mRNA-
513 76-cLNP compound.
514 Data in **Fig. 9 B** show a significant decrease in LPS induced neutrophil influx into the alveoli
515 after **s**ingle mRNA-76-cLNP treatment. We did not observe changes in LPS induced vascular
516 leakage (e.g., changes in wet lung weights) with mRNA-76-cLNP when compared to control
517 mRNA formulation in this model. These data may indicate that vascular leakage and leucocyte
518 extravasation do not necessarily occur together in blood vessel of the lung, which has been
519 discussed previously by others (Filewod and Lee 2019). Generally, these findings in murine
520 models for LPS-induced lung injury may also depend on the time point at which samples are
521 obtained and the corresponding physiological data are captured. In contrast to the IPML
522 model for primarily addressing vascular leakage, the LPS model might be not adequate for
523 simultaneously addressing both neutrophil efflux and lung edema at 24 h post endotoxin
524 challenge.
525 Intravenous mRNA-76-cLNP treatment was shown to intervene with leukocyte and in
526 particular neutrophil extravasation into the alveoli after LPS challenge. It should be noted
527 however, that the reduction of the influx of leukocytes in addition to a reduction in edema
528 formation might be clinically highly desirable to counteract the delayed apoptosis of
529 parenchymal neutrophils believed to contribute to tissue injury (Teder et al. 2002).
530 Taken together the data in our IPML mouse model demonstrate a dose dependent therapeutic
531 effect of mRNA-76-cLNP regarding endothelial permeability, while the LPS-induced pulmonary
532 neutrophilia mouse model depicted in **Fig. 9**. shows therapeutic efficacy on dysregulated lung
533 inflammation. Both underlying pathophysiological mechanisms, namely loss of endothelial
534 permeability and dysregulated lung inflammation, are hallmark events at the onset of early/
535 mild ARDS.
536 Thus, the advantage of our novel mRNA-76-cLNP compound as described above is its ability
537 to act in a highly spatially restricted manner thereby enabling the Tie2 agonist to rapidly and
538 almost exclusively target specifically that site of the endothelial capillary bed where the
539 pathophysiological lung edema occurs. This particular strong spatial restriction of action of
540 our mRNA compound enables a more rapid onset of Tie2 pathway activation, as well as
541 improved pharmacodynamics, compared to those drug modalities which require a more

542 continuous treatment due to the rapid clearance of recombinant proteins from the systemic
543 circulation.
544 Increased Ang2 levels were also found more recently to be strongly associated with COVID-19
545 in-hospital mortality and with non-resolving pulmonary condition (Villa et al. 2021a). Thus,
546 Ang2 may be an early and useful predictor and biomarker for patient stratification and of the
547 clinical course of COVID-19, and impending Ang2 binding a potential treatment option against
548 COVID-19 (Villa et al. 2021b). Moreover, inhibition of the antagonistic Ang2 or a transient and
549 localized upregulation of Ang1 -or a hyperactive derivative thereof- is a promising strategy to
550 restore Tie2 signaling in order to stabilize the barrier function and to prevent the inflammatory
551 lung leakage in ARDS/COVID-19 patients. With the understanding that the angiopoietin/Tie
552 (Ang/Tie) family has an established role in vascular physiology in regulating angiogenesis,
553 vascular permeability, and inflammatory responses, our data corroborate effectiveness and
554 mode of action of the clinical approach of treating damage of the lung vascular epithelium
555 with transient expression of an mRNA-LNP modality. The highly specific targeting of our
556 respective COMP-Ang1 cationic LNP of the lung vasculature thus enables spatially highly
557 restricted expression of COMP-Ang-1 for treating edema formation in ARDS patients as a new
558 treatment modality for further development.
559

## References


Aranda-Valderrama P, Kaynar AM. 2018. The Basic Science and Molecular Mechanisms of Lung Injury and Acute Respiratory Distress Syndrome. *International anesthesiology clinics* **56**: 1. /pmc/articles/PMC7680967/ (Accessed September 27, 2022).

Bogdanovic E, Nguyen VP, Dumont DJ. 2006. Activation of Tie2 by angiopoietin-1 and angiopoietin-2 results in their release and receptor internalization. *J Cell Sci* **119**: 3551–3560. https://www.ncbi.nlm.nih.gov/pubmed/16895971.

Calfee CS, Gallagher D, Abbott J, Thompson BT, Matthay MA. 2012. Plasma angiopoietin-2 in clinical acute lung injury: prognostic and pathogenetic significance. *Critical care medicine* **40**: 1731–1737. https://pubmed.ncbi.nlm.nih.gov/22610178/ (Accessed September 27, 2022).

Cho CH, Kammerer RA, Lee HJ, Steinmetz MO, Ryu YS, Lee SH, Yasunaga K, Kim KT, Kim I, Choi HH, et al. 2004a. COMP-Ang1: A designed angiopoietin-1 variant with nonleaky angiogenic activity. *Proceedings of the National Academy of Sciences of the United States of America* **101**: 5547–5552. https://www.pnas.org/doi/abs/10.1073/pnas.0307574101 (Accessed September 26, 2022).

Cho CH, Kammerer RA, Lee HJ, Yasunaga K, Kim KT, Choi HH, Kim W, Kim SH, Park SK, Lee GM, et al. 2004b. Designed angiopoietin-1 variant, COMP-Ang1, protects against radiation-induced endothelial cell apoptosis. *Proceedings of the National Academy of Sciences of the United States of America* **101**: 5553–5558. https://www.pnas.org/doi/abs/10.1073/pnas.0307575101 (Accessed September 26, 2022).

Diamond JM, Porteous MK, Cantu E, Meyer NJ, Shah RJ, Lederer DJ, Kawut SM, Lee J, Bellamy SL, Palmer SM, et al. 2012. Elevated plasma angiopoietin-2 levels and primary graft dysfunction after lung transplantation. *PloS one* **7**. https://pubmed.ncbi.nlm.nih.gov/23284823/ (Accessed September 27, 2022).

Dolinay T, Kim YS, Howrylak J, Hunninghake GM, An CH, Fredenburgh L, Massaro AF, Rogers A, Gazourian L, Nakahira K, et al. 2012. Inflammasome-regulated cytokines are critical mediators of acute lung injury. *American journal of respiratory and critical care medicine* **185**: 1225–1234. https://pubmed.ncbi.nlm.nih.gov/22461369/ (Accessed September 27, 2022).

Elbrecht DH, Long CJ, Hickman JJ. 2016. Transepithelial/endothelial Electrical Resistance (TEER) theory and ap-plications for microfluidic body-on-a-chip devices Keywords TEER Body-on-a-chip Barrier tissue Blood-brain barrier Organ Endothelial cells Epithelial cells Human-on-a-chip. *J Rare Dis Res Treat* **1**: 46–52. www.rarediseasesjournal.com (Accessed September 28, 2022).

Eygeris Y, Gupta M, Kim J, Sahay G. 2022. Chemistry of Lipid Nanoparticles for RNA Delivery. *Acc Chem Res* **55**: 2–12. https://www.ncbi.nlm.nih.gov/pubmed/34850635.

Fan E, Brodie D, Slutsky AS. 2018. Acute Respiratory Distress Syndrome: Advances in Diagnosis and Treatment. *JAMA* **319**: 698–710. https://jamanetwork.com/journals/jama/fullarticle/2673154 (Accessed September 27, 2022).

Fehring V, Schaeper U, Ahrens K, Santel A, Keil O, Eisermann M, Giese K, Kaufmann J. 2014. Delivery of therapeutic siRNA to the lung endothelium via novel Lipoplex formulation DACC. *Molecular therapy : the journal of the American Society of Gene Therapy* **22**: 811–

606 820. https://pubmed.ncbi.nlm.nih.gov/24390281/ (Accessed September 26, 2022).
607 Filewod NC, Lee WL. 2019. Inflammation without Vascular Leakage. Science Fiction No
608 Longer? *Am J Respir Crit Care Med* **200**: 1472–1476.
609 https://www.ncbi.nlm.nih.gov/pubmed/31381867.
610 Gallagher DC, Bhatt RS, Parikh SM, Patel P, Seery V, McDermott DF, Atkins MB, Sukhatme
611 VP. 2007. Angiopoietin 2 is a potential mediator of high-dose interleukin 2-induced
612 vascular leak. *Clinical cancer research : an official journal of the American Association*
613 *for Cancer Research* **13**: 2115–2120. https://pubmed.ncbi.nlm.nih.gov/17404094/
614 (Accessed September 27, 2022).
615 Gallagher DC, Parikh SM, Balonov K, Miller A, Gautam S, Talmor D, Sukhatme VP. 2008.
616 Circulating angiopoietin 2 correlates with mortality in a surgical population with acute
617 lung injury/adult respiratory distress syndrome. *Shock (Augusta, Ga)* **29**: 656–661.
618 https://pubmed.ncbi.nlm.nih.gov/18091573/ (Accessed September 27, 2022).
619 Ghosh CC, David S, Zhang R, Berghelli A, Milam K, Higgins SJ, Hunter J, Mukherjee A, Wei Y,
620 Tran M, et al. 2016. Gene control of tyrosine kinase TIE2 and vascular manifestations of
621 infections. *Proc Natl Acad Sci U S A* **113**: 2472–2477.
622 https://www.ncbi.nlm.nih.gov/pubmed/26884170.
623 Giaever I, Keese CR. 1993. A morphological biosensor for mammalian cells. *Nature* **366**: 591–
624 592. https://www.ncbi.nlm.nih.gov/pubmed/8255299 (Accessed September 29, 2022).
625 Gillich A, Zhang F, Farmer CG, Travaglini KJ, Tan SY, Gu M, Zhou B, Feinstein JA, Krasnow MA,
626 Metzger RJ. 2020. Capillary cell-type specialization in the alveolus. *Nature* **586**: 785–
627 789. https://www.ncbi.nlm.nih.gov/pubmed/33057196.
628 Gutbier B, Jiang X, Dietert K, Ehrler C, Lienau J, Van Slyke P, Kim H, Hoang VC, Maynes JT,
629 Dumont DJ, et al. 2017. Vasculotide reduces pulmonary hyperpermeability in
630 experimental pneumococcal pneumonia. *Critical Care* **21**.
631 Gutbier B, Neuhauß AK, Reppe K, Ehrler C, Santel A, Kaufmann J, Scholz M, Weissmann N,
632 Morawietz L, Mitchell TJ, et al. 2018. Prognostic and pathogenic role of angiopoietin-1
633 and -2 in pneumonia. *American Journal of Respiratory and Critical Care Medicine* **198**:
634 220–231. https://pubmed.ncbi.nlm.nih.gov/29447449/ (Accessed June 20, 2022).
635 Hashimoto T, Wu Y, Boudreau N, Li J, Matsumoto M, Young W. 2004. Regulation of tie2
636 expression by angiopoietin--potential feedback system. *Endothelium* **11**: 207–210.
637 https://www.ncbi.nlm.nih.gov/pubmed/15370298.
638 Hou X, Zaks T, Langer R, Dong Y. 2021. Lipid nanoparticles for mRNA delivery. *Nat Rev Mater*
639 **6**: 1078–1094. https://www.ncbi.nlm.nih.gov/pubmed/34394960.
640 Kauffman KJ, Webber MJ, Anderson DG. 2016. Materials for non-viral intracellular delivery of
641 messenger RNA therapeutics. *J Control Release* **240**: 227–234.
642 https://www.ncbi.nlm.nih.gov/pubmed/26718856.
643 Keddissi JI, Youness HA, Jones KR, Kinasewitz GT. 2019. Fluid management in Acute
644 Respiratory Distress Syndrome: A narrative review. *Canadian Journal of Respiratory*
645 *Therapy: CJRT = Revue Canadienne de la Thérapie Respiratoire : RCTR* **55**: 1.
646 /pmc/articles/PMC6591787/ (Accessed September 28, 2022).
647 Khan KA, Wu FT, Cruz-Munoz W, Kerbel RS. 2021. Ang2 inhibitors and Tie2 activators:
648 potential therapeutics in perioperative treatment of early stage cancer. *EMBO Mol Med*
649 **13**: e08253. https://www.ncbi.nlm.nih.gov/pubmed/34125494.
650 Kowalski PS, Rudra A, Miao L, Anderson DG. 2019. Delivering the Messenger: Advances in
651 Technologies for Therapeutic mRNA Delivery. *Mol Ther* **27**: 710–728.
652 https://www.ncbi.nlm.nih.gov/pubmed/30846391.
653 Leppänen VM, Saharinen P, Alitalo K. 2017. Structural basis of Tie2 activation and Tie2/Tie1

654 heterodimerization. *Proceedings of the National Academy of Sciences of the United*
655 *States of America* **114**: 4376–4381.
656 https://www.pnas.org/doi/abs/10.1073/pnas.1616166114 (Accessed October 10,
657 2022).
658 Matthay MA, Zemans RL, Zimmerman GA, Arabi YM, Beitler JR, Mercat A, Herridge M,
659 Randolph AG, Calfee CS. 2019. Acute respiratory distress syndrome. *Nature Reviews*
660 *Disease Primers 2019 5:1* **5**: 1–22. https://www.nature.com/articles/s41572-019-0069-0
661 (Accessed August 4, 2022).
662 McCarter SD, Mei SHJ, Lai PFH, Qiu WZ, Parker CH, Suen RS, Hood RD, Zhao YD, Deng Y, Han
663 RNN, et al. 2007. Cell-based angiopoietin-1 gene therapy for acute lung injury. *American*
664 *journal of respiratory and critical care medicine* **175**: 1014–1026.
665 https://pubmed.ncbi.nlm.nih.gov/17322110/ (Accessed September 28, 2022).
666 Meyer NJ, Gattinoni L, Calfee CS. 2021. Acute respiratory distress syndrome. *The Lancet* **398**:
667 622–637. https://pubmed.ncbi.nlm.nih.gov/34217425/ (Accessed October 6, 2022).
668 Mitchell TJ, Walker JA, Saunders FK, Andrew PW, Boulnois GJ. 1989. Expression of the
669 pneumolysin gene in Escherichia coli: rapid purification and biological properties.
670 *Biochimica et biophysica acta* **1007**: 67–72. https://pubmed.ncbi.nlm.nih.gov/2642385/
671 (Accessed September 29, 2022).
672 Oh N, Kim K, Kim SJ, Park I, Lee JE, Seo YS, An HJ, Kim HM, Koh GY. 2015. A Designed
673 Angiopoietin-1 Variant, Dimeric CMP-Ang1 Activates Tie2 and Stimulates Angiogenesis
674 and Vascular Stabilization in N-glycan Dependent Manner. *Sci Rep* **5**: 15291.
675 https://www.ncbi.nlm.nih.gov/pubmed/26478188.
676 Parikh SM, Mammoto T, Schultz A, Yuan HT, Christiani D, Karumanchi SA, Sukhatme VP.
677 2006. Excess circulating angiopoietin-2 may contribute to pulmonary vascular leak in
678 sepsis in humans. *PLoS medicine* **3**: 356–370.
679 https://pubmed.ncbi.nlm.nih.gov/16417407/ (Accessed September 28, 2022).
680 Saharinen P, Eklund L, Alitalo K. 2017a. Therapeutic targeting of the angiopoietin–TIE
681 pathway. *Nature Reviews Drug Discovery 2017 16:9* **16**: 635–661.
682 https://www.nature.com/articles/nrd.2016.278 (Accessed September 26, 2022).
683 Saharinen P, Leppanen VM, Alitalo K. 2017b. SnapShot: Angiopoietins and Their Functions.
684 *Cell* **171**: 724-724 e1. https://www.ncbi.nlm.nih.gov/pubmed/29053972.
685 Santel A, Aleku M, Keil O, Endruschat J, Esche V, Durieux B, Loffler K, Fechtner M, Rohl T,
686 Fisch G, et al. 2006a. RNA interference in the mouse vascular endothelium by systemic
687 administration of siRNA-lipoplexes for cancer therapy. *Gene Ther* **13**: 1360–1370.
688 https://www.ncbi.nlm.nih.gov/pubmed/16625242.
689 Santel A, Aleku M, Keil O, Endruschat J, Esche V, Fisch G, Dames S, Loffler K, Fechtner M,
690 Arnold W, et al. 2006b. A novel siRNA-lipoplex technology for RNA interference in the
691 mouse vascular endothelium. *Gene Ther* **13**: 1222–1234.
692 https://www.ncbi.nlm.nih.gov/pubmed/16625243.
693 Seybold J, Thomas D, Witzenrath M, Boral Ş, Hocke AC, Bürger A, Hatzelmann A, Tenor H,
694 Schudt C, Krüll M, et al. 2005. Tumor necrosis factor-α–dependent expression of
695 phosphodiesterase 2: role in endothelial hyperpermeability. *Blood* **105**: 3569–3576.
696 https://ashpublications.org/blood/article/105/9/3569/21288/Tumor-necrosis-factor-
697 dependent-expression-of (Accessed September 29, 2022).
698 Srinivasan B, Kolli AR, Esch MB, Abaci HE, Shuler ML, Hickman JJ. 2015. TEER measurement
699 techniques for in vitro barrier model systems. *Journal of laboratory automation* **20**:
700 107–126. https://pubmed.ncbi.nlm.nih.gov/25586998/ (Accessed September 28, 2022).
701 Tabruyn SP, Colton K, Morisada T, Fuxe J, Wiegand SJ, Thurston G, Coyle AJ, Connor J,

McDonald DM. 2010. Angiopoietin-2-Driven Vascular Remodeling in Airway Inflammation. *The American Journal of Pathology* **177**: 3233. /pmc/articles/PMC2993300/ (Accessed September 27, 2022).

Teder P, Vandivier RW, Jiang D, Liang J, Cohn L, Pure E, Henson PM, Noble PW. 2002. Resolution of lung inflammation by CD44. *Science* **296**: 155–158. https://www.ncbi.nlm.nih.gov/pubmed/11935029.

Thurston G, Rudge JS, Ioffe E, Zhou H, Ross L, Croll SD, Glazer N, Holash J, McDonald DM, Yancopoulos GD. 2000. Angiopoietin-1 protects the adult vasculature against plasma leakage. *Nature medicine* **6**: 460–463. https://pubmed.ncbi.nlm.nih.gov/10742156/ (Accessed September 27, 2022).

Thurston G, Suri C, Smith K, McClain J, Sato TN, Yancopoulos GD, McDonald DM. 1999. Leakage-resistant blood vessels in mice transgenically overexpressing angiopoietin-1. *Science (New York, NY)* **286**: 2511–2514. https://pubmed.ncbi.nlm.nih.gov/10617467/ (Accessed September 27, 2022).

Tiruppathi C, Malik AB, Del Vecchio PJ, Keese CR, Glaever I. 1992. Electrical method for detection of endothelial cell shape change in real time: assessment of endothelial barrier function. *Proceedings of the National Academy of Sciences of the United States of America* **89**: 7919. /pmc/articles/PMC49826/?report=abstract (Accessed September 29, 2022).

Van Der Heijden M, Van Nieuw Amerongen GP, Koolwijk P, Van Hinsbergh VWM, Groeneveld ABJ. 2008. Angiopoietin-2, permeability edema, occurrence and severity of ALI/ARDS in septic and non-septic critically ill patients. *Thorax* **63**: 903–909. https://pubmed.ncbi.nlm.nih.gov/18559364/ (Accessed September 27, 2022).

Villa E, Critelli R, Lasagni S, Melegari A, Curatolo A, Celsa C, Romagnoli D, Melegari G, Pivetti A, Di Marco L, et al. 2021a. Dynamic angiopoietin-2 assessment predicts survival and chronic course in hospitalized patients with COVID-19. *Blood Adv* **5**: 662–673. https://www.ncbi.nlm.nih.gov/pubmed/33560382 (Accessed September 27, 2022).

Villa E, Critelli R, Lasagni S, Melegari A, Curatolo A, Celsa C, Romagnoli D, Melegari G, Pivetti A, Di Marco L, et al. 2021b. Dynamic angiopoietin-2 assessment predicts survival and chronic course in hospitalized patients with COVID-19. *Blood Adv* **5**: 662–673. https://www.ncbi.nlm.nih.gov/pubmed/33560382.

Von Bethmann AN, Brasch F, Nüsing R, Vogt K, Volk HD, Müller KM, Wendel A, Uhlig S. 1998. Hyperventilation induces release of cytokines from perfused mouse lung. *American journal of respiratory and critical care medicine* **157**: 263–272. https://pubmed.ncbi.nlm.nih.gov/9445308/ (Accessed September 29, 2022).

Wallace RG, Rochfort KD, Barabas P, Curtis TM, Uehara H, Ambati BK, Cummins PM. 2021. COMP-Ang1: Therapeutic potential of an engineered Angiopoietin-1 variant. *Vascul Pharmacol* **141**: 106919. https://www.ncbi.nlm.nih.gov/pubmed/34583025.

Wehrle C, Van Slyke P, Dumont DJ. 2009. Angiopoietin-1-induced ubiquitylation of Tie2 by c-Cbl is required for internalization and degradation. *Biochem J* **423**: 375–380. https://www.ncbi.nlm.nih.gov/pubmed/19689429.

Witzenrath M, Gutbier B, Hocke AC, Schmeck B, Hippenstiel S, Berger K, Mitchell TJ, De Los Toyos JR, Rosseau S, Suttorp N, et al. 2006. Role of pneumolysin for the development of acute lung injury in pneumococcal pneumonia. *Critical Care Medicine* **34**: 1947–1954.

Wu FT, Lee CR, Bogdanovic E, Prodeus A, Gariépy J, Kerbel RS. 2015. Vasculotide reduces endothelial permeability and tumor cell extravasation in the absence of binding to or agonistic activation of Tie2. *EMBO molecular medicine* **7**: 770–787. https://pubmed.ncbi.nlm.nih.gov/25851538/ (Accessed September 29, 2022).

750 **Figure 1**

751

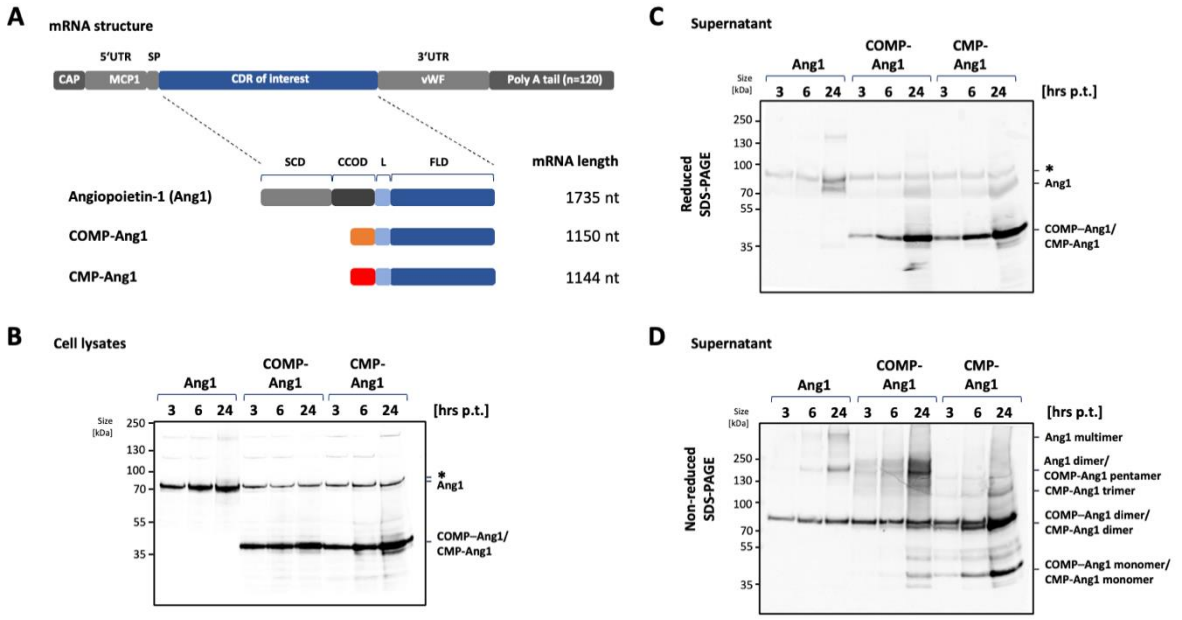


752
753
754

755 **Figure 1: mRNA directed expression, secretion and multimerization of human Ang1,**

756 **COMP-Ang-1 and CMP-Ang1 *in vitro*.**

757 **(A)** General structure of mRNA with signal peptide (SP) sequence flanked by designated 5´-
758 and 3´- UTR regions plus defined polyA-tail. Schematic representation of protein domain
759 structure of the natural protein Ang1 and the derived engineered humanized fusion proteins
760 COMP-Ang1 and CMP-Ang1 according to Cho et al.,2004 and Oh et al., 2015. Protein domains
761 of human Ang1: SCD, super clustering domain; CCOD, coiled coil domain; L, linker; FLD,
762 Fibrinogen-related domain; the multimerization domains of COMP (orange) and of CMP
763 protein (red) are indicated. **(B)** Expression, **(C)** secretion and **(D)** multimerization of wt Ang1
764 and Ang1 derivates in Hela cells. Cells were transfected for 2 h with mRNA-52 encoding Ang1,
765 mRNA-76 encoding COMP-Ang1, or mRNA-59 encoding CMP-Ang1. Cell lysates and
766 supernatants were harvested at indicated time points post transfection (p.t.) and analyzed by
767 Western blotting using Ang1-specific antibody. (*, unidentified band)

768

769 **Figure 2**

770

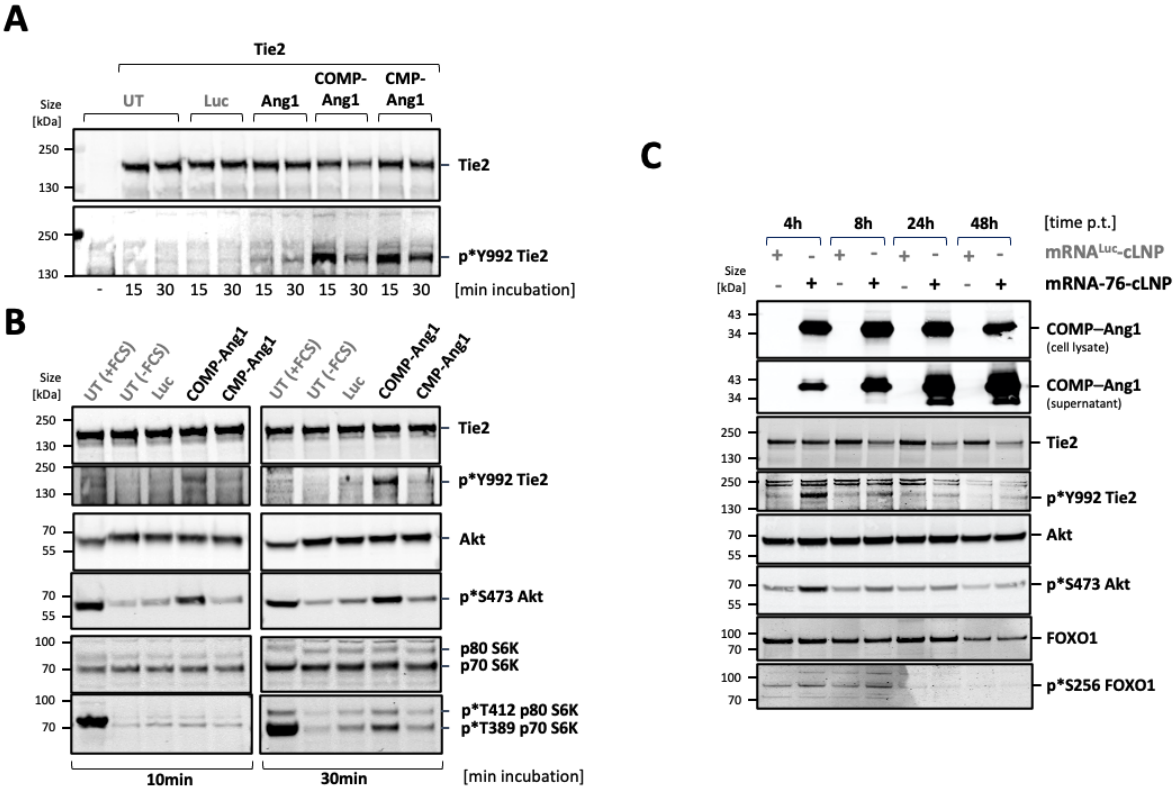


771
772
773

774 **Figure 2: Activation of Tie2 pathway by Ang1, COMP-Ang1 and CMP-Ang1 containing**
775 **supernatants**

776 **(A)** Immunoblot of Tie2 expression and Tie2 phosphorylation from Tie2-expressing Hela cells
777 after 15 or 30 min incubation with supernatant from HeLa cells expressing Luc, Ang1, COMP-
778 Ang1 and CMP-Ang-1 (see Fig. 1) following incubation with supernatants from Hela cells
779 transfected for 24h with Luc-mRNA or mRNA-52 encoding Ang1, mRNA-76 encoding COMP-
780 Ang1, and mRNA-59 encoding CMP-Ang1. **(B)** Activation of Tie2 pathway in serum-starved
781 primary human pulmonary microvascular endothelial cells (HPMEC) by COMP-Ang1 and by
782 CMP-Ang1 containing supernatant from mRNA-76 or mRNA-59 transfected HeLa cells. Tie2-
783 pathway activation is demonstrated by analysis of Tie2 phosphorylation status and by
784 presence of phosphorylation at the downstream effectors Akt and S6K. **(C)** Tie2-pathway
785 activation after transfection of LNP-formulated, COMP-Ang1-encoding mRNA-76 in serum-
786 starved HPMEC. COMP-Ang1 expression, secretion, Tie2, Akt, and FOXO1 phosphorylation is
787 shown by immunoblot on cell lysates at different time points post transfection (p.t.). (UT,
788 untreated; FCS, Fetal calf serum; Luc, control Nano-Luciferase-encoding mRNA).

789

790 **Figure 3**

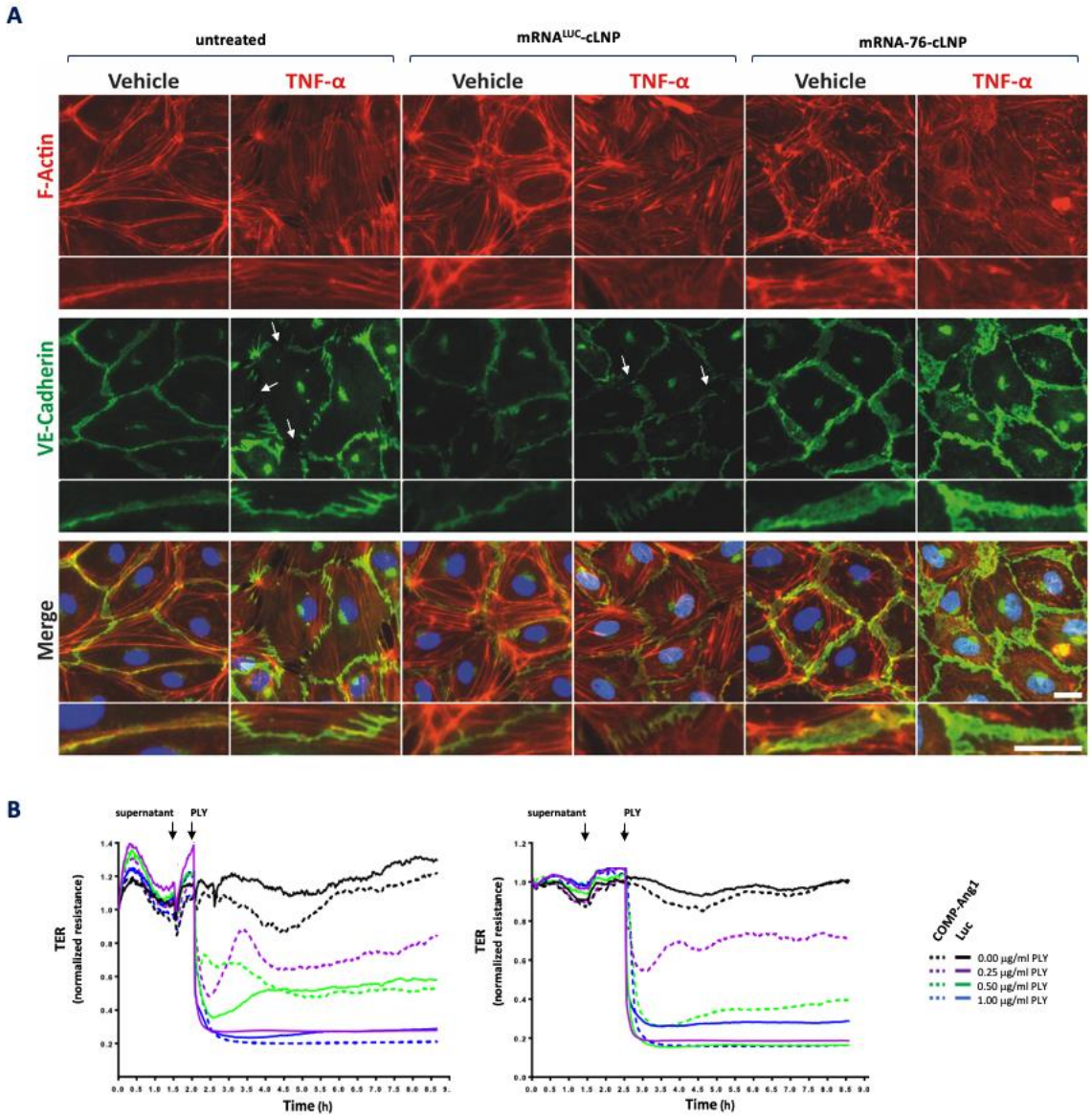


791

792

793 **Figure 3: Cell staining by immunofluorescence demonstrating stabilization of endothelial**

794 **adherens junctions.**

795 **(A)** Effect of COMP-Ang1 on F-actin remodeling and VE-Cadherin distribution in isolated

796 human pulmonary microvascular endothelial cell. HPMECs grown on glass coverslips were

797 transfected for 24h with control mRNA$^{LUC}$ or with mRNA-76 encoding COMP-Ang1 with or

798 without temporal addition of 10 ng/ml TNF$\alpha$, followed by immunofluorescence staining with

799 VE-Cadherin-specific antibody and with Alexa Fluor 594 phalloidin to detect actin filaments.

800 Arrows indicate disrupted VE-Cadherin complexes. **B)** Transcellular electrical resistance (TER)

801 measurements of HPMEC monolayers. HPMEC were incubated for 30 min (top) or 60 min

802 (bottom) with supernatant from mRNA-76 or with $mRNA^{LUC}$ (Luciferase) and the treated with
803 supernatants from Hela cells transfected for 24 h with control $mRNA^{LUC}$ or mRNA-76 encoding
804 COMP-Ang1 and stimulated with indicated amount of pneumolysin (PLY; 0.25, 0.5, 0.75,
805 1.0 µg/ml). PLY stimulation decreased TER of HPMEC monolayers, displaying loss of
806 endothelial integrity when incubated with control Luciferase supernatant (solid curve).
807 Preincubation with COMP-Ang1 containing supernatant attenuated the PLY-induced TER
808 decrease (purple lines dashed versus solid).
809
810
811
812
813
814
815
816
817
818
819
820
821
822
823
824
825
826
827
828
829
830
831
832

833 **Figure 4**

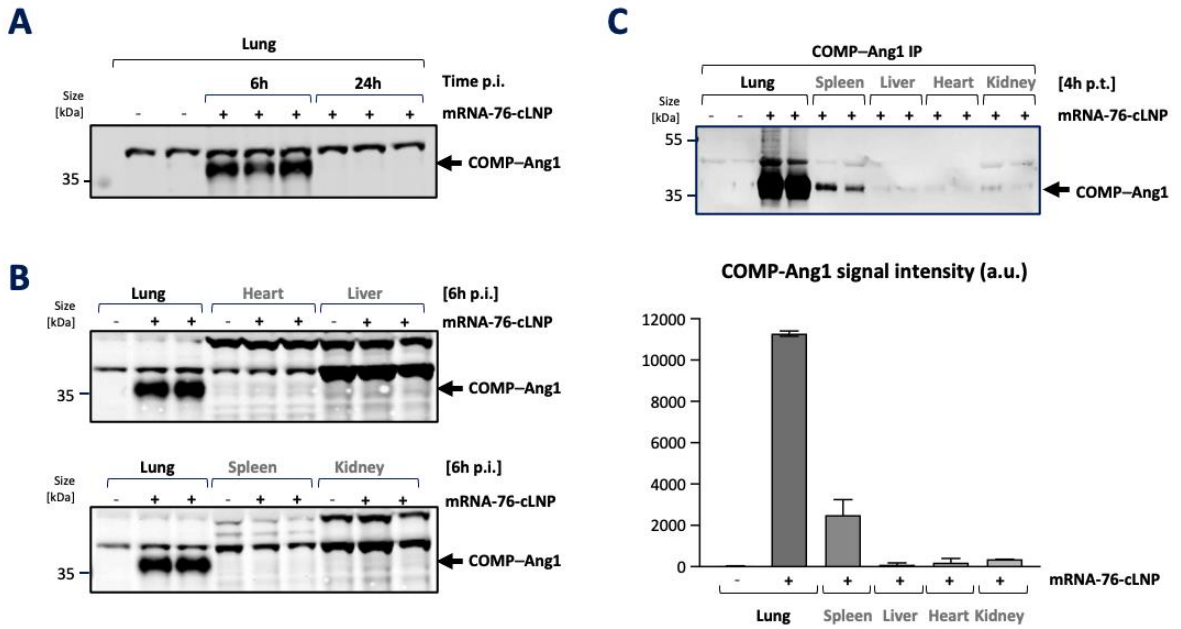


834

835 **Figure 4. Transient expression of COMP-Ang1 in murine lungs by cLNP-mediated lung**
836 **delivery of mRNA-76**

837 **(A)** Immunoblot of lung tissue lysates 6 and 24 h after administration of 1.5 mg/kg mRNA-76-
838 cLNP (+) or saline control (-). The expressed COMP-Ang1 fusion protein is indicated by an
839 arrow. **(B)** Immunoblot of different tissue lysates 6h post-administration of 1.5 mg/kg mRNA-
840 76-cLNP (+) or saline control (-). Lung selective COMP-Ang1 protein is indicated by an arrow.
841 **(C)** Immunoprecipitation of COMP-Ang1 protein using Tie2-Fc-coupled magnetic beads from
842 indicated tissue samples 4 h after administration of 1.5 mg mRNA-76-cLNP (+) or saline control
843 (-).

844

845

846

847

848

**Figure 5**

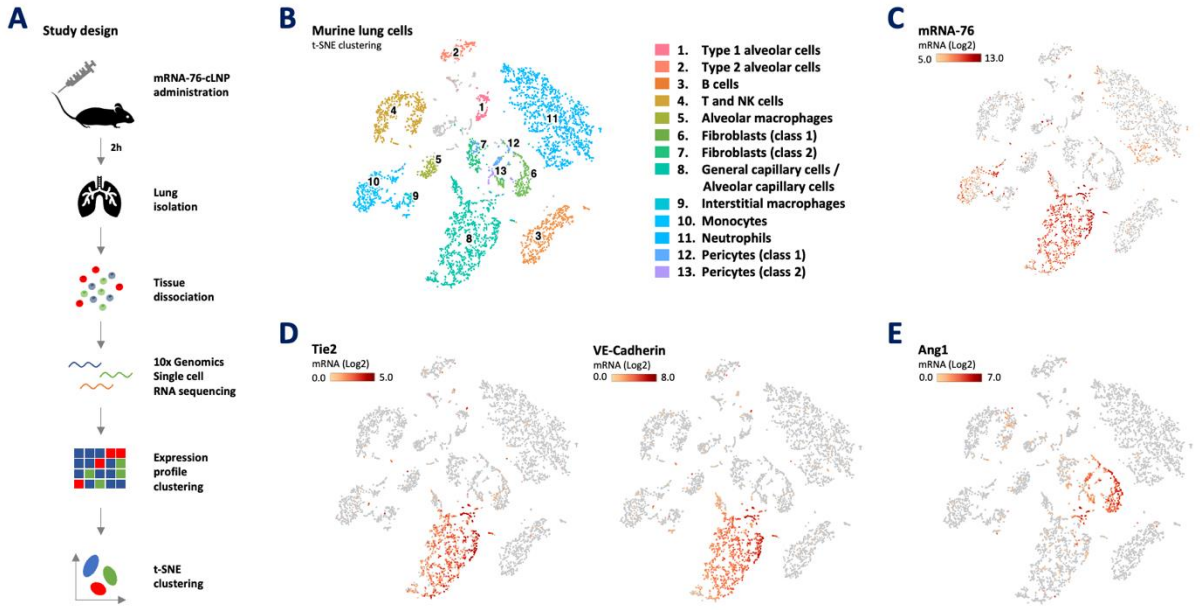


**Figure 5: cLNP-mediated delivery of 1.5 mg/kg mRNA-76 leads to uptake predominantly in murine pulmonary capillary endothelial cells.**

**(A)** Experimental design and workflow (**B**) Loupe-based t-distributed stochastic neighbor embedding (t-SNE) clustering of murine lung cell types clustered by single-cell transcriptional analysis of 5,100 cells after quality control, showing a total of 13 distinct cell type clusters as indicated by numbers. **(C)** t-SNE plots showing levels for COMP-Ang1-encoding mRNA-76. **(D)** t-SNE plots showing levels for canonical markers of endothelial cells (Tie2, VE-Cadherin). **(F)** cells expressing Ang1 (pericytes class 1 and 2, fibroblasts class 1). The intensity of expression is indicated by red coloring.

869 **Figure 6**

870

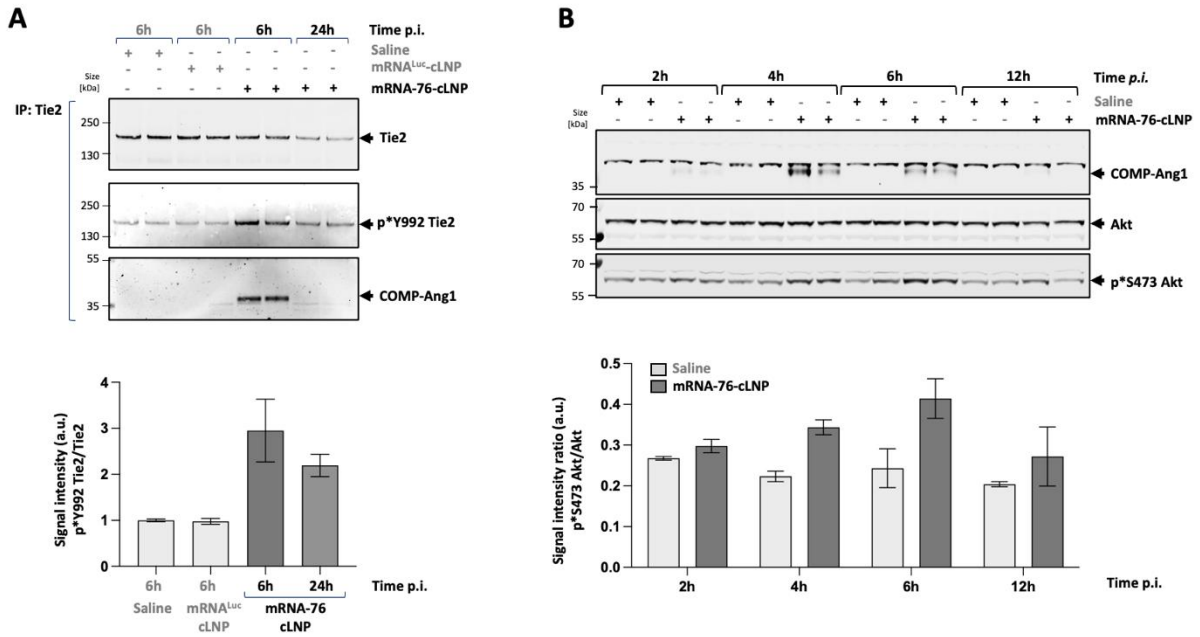


871

872

873 **Figure 6: cLNP-mediated delivery of mRNA-76 leads to time-dependent Tie2 pathway**

874 **activation *in vivo*.**

875 **(A)** Immunoblot after immunoprecipitation of murine Tie2 from lung samples at indicated

876 time points after i.v. administration of 1.5 mg/kg mRNA-76-cLNP. **(B)** Immunoblot of murine

877 lunge tissue lysates analyzing COMP-Ang1 expression level and Akt phosphorylation status at

878 indicated time points after i.v. administration of 1.5 mg/kg mRNA-76-cLNP or Saline.

879

880

881

882

883

884

885

886

887

888

889

890

**Figure 7**

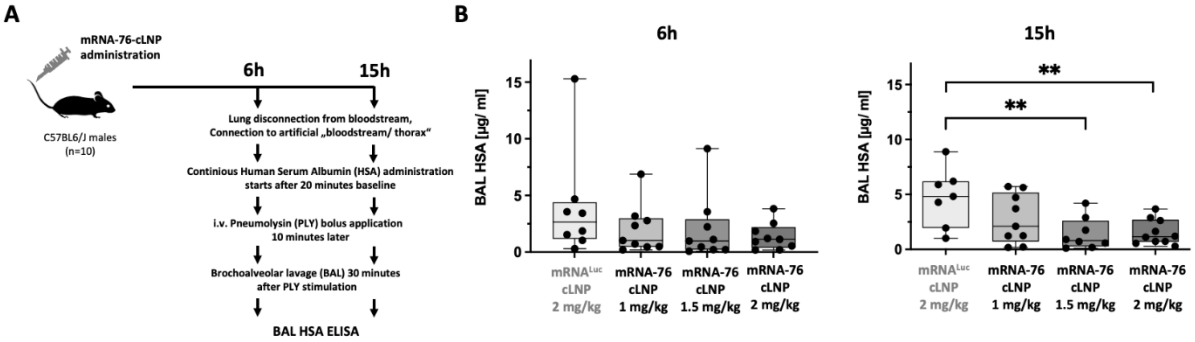


**Figure 7: Systemic mRNA-76 treatment stabilized endothelial barrier lung function in an *ex vivo* isolated perfused and ventilated mouse lung (IPML) model.**

**(A)** Schematic diagram of the experimental protocol of the *ex vivo* perfused and ventilated mouse lung model. 6 h, 15 h after administration of mRNA-76-cLNP (1, 1.5 and 2 mg/kg) or control $mRNA^{LUC}$-LNP (2 mg/kg) lungs were isolated and stimulated with PLY (1.4 µg/ml) for 1 minute. After 30 min, lung vascular permeability was assessed by quantifying respective concentrations of continuously infused human serum albumin (HSA) in the bronchoalveolar lavage fluid (BALF). **(B)** Graphic showing treatment with mRNA-76 to significantly decrease pneumolysin-induced hyperpermeability of mouse lungs as compared to treatment with control $mRNA^{LUC}$-LNP 6 h (left) and 15 h (right) post mRNA-76-cLNP treatment as shown by HAS ELISA. Values are given as mean ($n$ = 10, **$p<0.01$ between indicated groups) concentration of human serum albumin (HSA) in bronchoalveolar lavage fluid (BALF). HSA concentration of individual mice are indicated as dots.

917 **Figure 8**

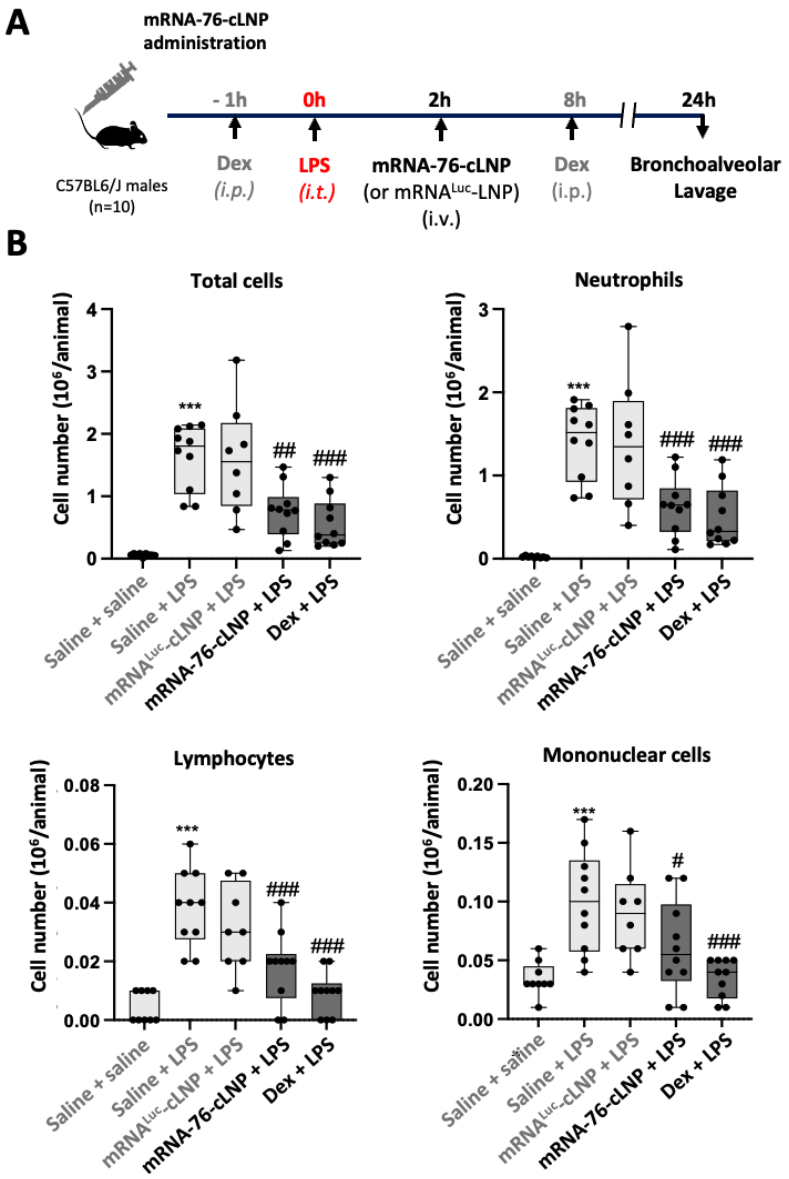


918

919

920 **Figure 8**: **LPS-induced Pulmonary Neutrophilia Mouse Model**

921 **(A)** Schematic drawing of the experimental protocol. Animals (n=10) were challenged
922 intratracheally with 0.9% w/v saline or LPS (3 mg/kg). A fixed volume of 50 µL, equal to an
923 approximate intratracheal dose volume of 2.5 mL/kg, based on a 20 g mouse, was applied
924 intratracheally. 2h after LPS administration mRNA-76-cLNP (1.5 mg/kg IV) or mRNA$^{LUC}$-cLNP01
925 (1.5 mg/kg IV) was intravenously administered, and bronchoalveolar lavage fluid (BALF) was
926 analysed after 24 h. **(B)** Effect of COMP-Ang1 expression on BALF total and differential cell
927 counts and on wet lung weight in a murine model of endotoxin (LPS)-induced pulmonary
928 inflammation. Data shown as mean ± standard error of the mean. *** $p$<0.001 when

compared to saline challenged control group. # $p<0.05$, ## $p<0.01$, ### $p<0.001$ as compared to LPS challenged and vehicle treated group.